

N-t-Butyl- α -aryl Nitrones as Potent Spin Traps: DFT Analysis of Electron Localization Function Topology, Local Selectivity, Reactivity and Solvent Effects

NIVEDITA ACHARJEE*^{ORCID} and SOURAV MONDAL

Department of Chemistry, Durgapur Government College, J.N. Avenue, Durgapur-713214, India

*Corresponding author: E-mail: nivchem@gmail.com

Received: 13 December 2019;

Accepted: 1 February 2020;

Published online: 29 April 2020;

AJC-19855

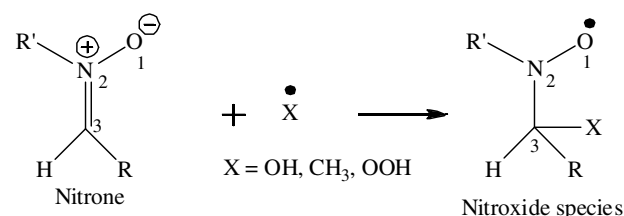
Density functional theory studies were performed to analyze the reactivity and selectivity of radical capture by *N-t*-butyl- α -aryl nitrones. Biologically relevant three important radicals *viz.* hydroxyl, methyl and hydroperoxyl were selected for the study. Topological analysis of the electron localization function (ELF) allows to classify these nitrones as zwitter-ionic type three atom components (TAC). Effects of electron withdrawing and electron donating *C*-aryl substituents on the electronic chemical potentials, global hardness, electrophilic and nucleophilic indices of nitrones were observed. Radical attack at the carbon atom was predicted by Merz-Kollman algorithm, which is in agreement with the experiments unlike the natural population analysis. Hydroxyl adducts were predicted to be more stable than methyl and hydroperoxyl adducts. *cis*-Adducts were more stable than the *trans*-, with the highest differences in stability noted for the methyl adducts. Relative energies of adducts was lowered in non-polar solvents and thus increase in stability was observed along the series from water to heptane.

Keywords: Spin trapping, Conceptual DFT, Nitrones, Free energy, Electron localization function, Merz-Kollman algorithm.

INTRODUCTION

Free radicals are generated in biological tissues by various cellular and molecular mechanisms [1]. Imbalance of free radicals and antioxidants in human body causes cellular injury and this radiation mediated cellular damage has been implicated in the pathogenesis of a wide spectrum of diseases such as cancer [2], neurodegeneration [3], cardiovascular [4] disorders *etc.* Spin traps [5] are used to detect and characterize free radicals in biological systems and have been widely regarded as therapeutic agents in biomedical research. Nitrones [6,7] are one of the important class of spin traps to show biological activity in various experimental models. Nitrones capture primary radicals such as hydroxyl (OH[•]), methyl (CH₃[•]) and hydroperoxyl (HOO[•]) to form persistent nitroxide species (**Scheme-I**), which has ensured its applicability for biological systems.

In 1991, Kotake and Janzen [8] reported the mechanism for hydroxyl radical capture by *N-t*-butyl- α -phenyl nitrone (PBN) in water, while the stability of PBN-hydroxyl adducts were examined over a varied pH range [9]. Carbon atom was obtained as the favoured site for radical attack in these studies. A variety of cyclic nitrones such as 1-pyrroline-*N*-oxide (DMPO)



- R = Ph, R' = *t*-Bu (1)
R = 4-Methyl-phenyl, R' = *t*-Bu (2)
R = 4-Nitrophenyl, R' = *t*-Bu (3)
R = 4-Cyanophenyl, R' = *t*-Bu (4)
R = 4-Methoxyphenyl, R' = *t*-Bu (5)

Scheme-I: Radical capture by nitrones

[10] and 1,1,3-trimethyliso-indole-*N*-oxide (TMINO) [11] were subsequently developed as spin traps. However, the pharmacological action of PBN and its significant biological activity has crowned its trapping efficiency in the nitrone chemistry and several experimental studies have been devoted to establish its utility as a spin trap of biologically relevant free radicals. A decline of free radicals in isolated rat hearts was demonstrated by the use of PBN [12], while a medical

study reported by Lapchak and coworkers [13] highlighted the therapeutic benefit of PBN for the treatment of ischemic stroke. Polovyanenko *et al.* [14] studied the spin trapping of glutathyl radical (a major intracellular antioxidant in biological tissues) by PBN. Marchand *et al.* [15] used a cocktail of spin traps for free radicals in biological systems and PBN was one of the major components of this cocktail. In addition to pharmacological properties, the potential use of PBN as a spin trap to control reactive oxygen species (ROS) in antipollution cosmetics has been recently reviewed [16].

Several researchers have addressed the experimental aspects of spin trapping by PBN since the last two decades. However, theoretical investigations are quite limited in this field in comparison, namely the computational studies for spin trapping by cyclic nitrones [17-19]. With this in mind, the present study aims to provide a systematic DFT analysis of the electronic structure, substituent effects, reactivity and solvent effects on the spin trapping ability of *N-t*-butyl- α -phenyl nitron (PBN) and its α -aryl derivatives. Three biologically relevant free radicals, hydroxyl (OH \cdot), methyl (CH $_3\cdot$) and hydroperoxyl (HOO \cdot) have been selected for the present investigation. This report has been divided into four sections *viz.* (a) topological analysis of electron localization function [20,21] (ELF) of *N-t*-butyl- α -phenyl nitron (PBN) and its derivatives to establish a straightforward connection between the electronic structure and reactivity; (b) analysis of global indices defined within conceptual density functional theory (CDFT) [22]; (c) comparative analysis of the relative energy, enthalpy and free energy of the adducts and (d) analysis of solvent effects on the stability of adducts.

COMPUTATIONAL METHODS

Geometry optimization of the stationary points was carried out using B3LYP functional [23,24] together with the standard 6-31G(d) basis set with Berny's analytical optimization method [25,26]. Absence of imaginary frequency in the optimized stationary states was ensured through frequency calculations at the same level. Thermodynamic parameters of the adducts, energy, enthalpy and free energies were calculated relative to nitron and the radicals at 298 K and 1 atm. pressure. Solvent effects in water, DMSO, acetone, methanol, toluene, CH $_2$ Cl $_2$, CCl $_4$ and heptane were taken into account by single point calculations at the gas phase optimized structures using polarized continuum model (PCM) [27] within the framework of self consistent reaction field (SCRf) [28,29]. CDFT indices [22], namely the electronic chemical potential (μ), chemical hardness (η), electrophilicity (ω) and nucleophilicity (N) indices, Fukui functions $f^+(r)$, $f^-(r)$ and $f^o(r)$, respectively for electrophilic, nucleophilic and radical attack were calculated using the following formulae [22]:

$$\mu \approx \frac{(E_{\text{HOMO}} + E_{\text{LUMO}})}{2}$$

$$\eta \approx E_{\text{LUMO}} - E_{\text{HOMO}}$$

where E_{HOMO} and E_{LUMO} are the computed HOMO and LUMO energies of nitron.

$$\omega = \frac{\mu^2}{2\eta}$$

$$N = E_{\text{HOMO (Nucleophilic)}} - E_{\text{HOMO (TCE)}}$$

where, TCE denotes tetracyanoethylene, which is considered as the neutral species showing maximum electrophilic character.

$$f^+(r) \approx \rho_{N+1}(r) - \rho_{N_0}(r) \text{ (for nucleophilic attack)}$$

$$f^-(r) \approx \rho_{N_0}(r) - \rho_{N-1}(r) \text{ (for electrophilic attack)}$$

where $\rho_{N_0}(r)$, $\rho_{N-1}(r)$ and $\rho_{N+1}(r)$ are the atomic charges for species containing N (neutral), $N-1$ (cationic) and $N+1$ (anionic) number of electrons

$$f^o(r) \approx \frac{f^+(r) + f^-(r)}{2} \text{ (for radical attack)}$$

ELF topology of nitrones was calculated using Multiwfn [30] program and the basin-attractor positions were visualized using VMD software [31]. ELF localization domains were obtained using UCSF Chimera software [32]. All the calculations were performed using Gaussian 2003 program (Revision D. 01) [33].

RESULTS AND DISCUSSION

ELF topological analysis of *N-t*-butyl- α -aryl nitrones:

Becke and Edgecombe [20] proposed a concept of electron localization function (ELF) to reveal a clear picture of atomic shell structure-core, binding and lone pair of electrons in the molecular systems. Subsequently using ELF analysis, the chemical bonding was classified by Silvi and Savin [21]. The localization attractors in molecular systems can be classified into three types *viz.* bonding, core and non-bonding attractors. Bonding attractors indicate a shared electron pair interactions and are situated between the core attractors, while non-bonding attractors are associated with the non-bonding electron density, such as lone-pairs or *pseudoradical* centers. Monosynaptic basin, $V(A)$ is associated with the non-bonding electron density at atom A, while disynaptic basin $V(A,B)$ is associated with the bonding region between A and B.

Domingo *et al.* [34,35] classified the three atom components (TACs) as *pseudoradical* type (*pdr-type*), *pseudo(mono)radical* type (*pmr-type*), carbenoid type (*cb-type*) and zwitter-ionic type (*zw-type*) by ELF analysis. Monosynaptic basins integrating at a total electron density less than 1e are called *pseudoradical* centers, while monosynaptic basins integrating at a total electron density of about 2e in neutral molecules are called carbenoid centers. The three atom components (TACs) with one *pseudoradical* centre are called *pseudo(mono)radical* type (*pmr-type*), with two *pseudoradical* centres are called *pseudodiradical* type (*pdr-type*) and with a carbenoid centre are called *cb-type*. TACs with no *pseudoradical* or carbenoid centers are called zwitter-ionic type TACs, which is different from the concept of zwitter-ionic structure generally used for chemical structures. This classification of electronic structure has allowed assessment of the reactivity of TACs in cycloadditions [35], which follows the order *pdr-type* > *pmr-type* ~ *cb-type* > *zw-type*.

Nitron is a TAC and therefore, a topological analysis of nitrones **1-5** was performed in this study to understand the electronic structure and reactivity. The most significant ELF valence basin populations of nitrones are given in Table-1, while ELF localization domains and ELF attractors are shown in Figs. 1 and 2. Nitrones **1-5** showed the presence of mono-

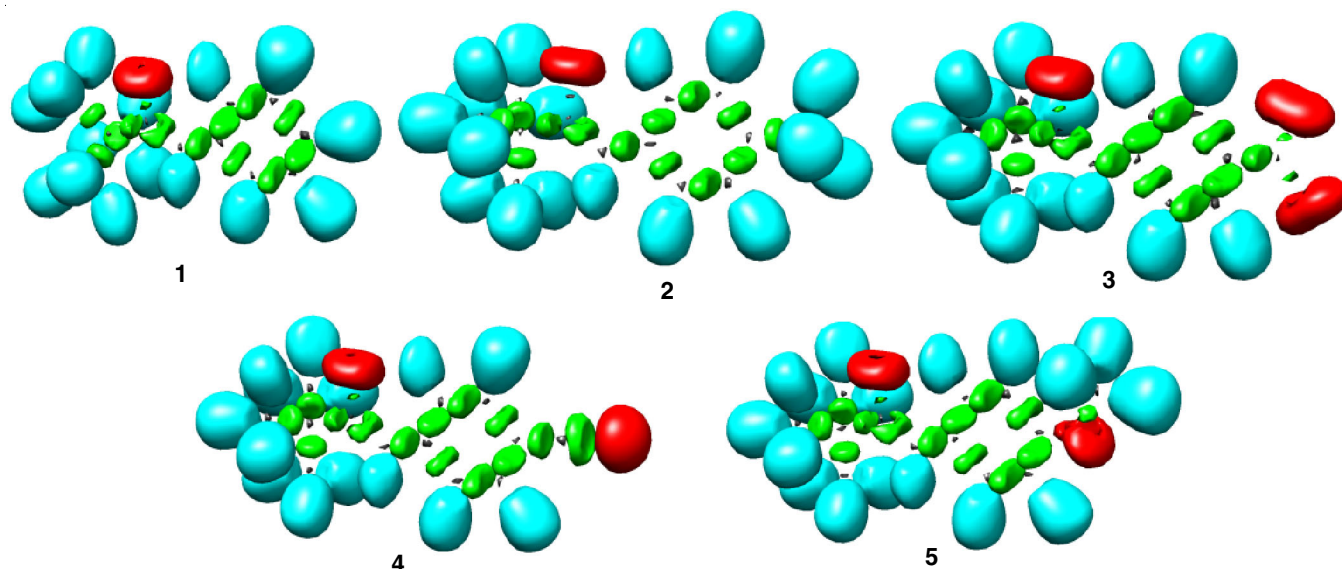


Fig. 1. ELF localization domains [Isovalue: 0.79] of nitrones **1-5**. Protonated basins are shown in blue, disynaptic basins are shown in green, monosynaptic basins are shown in red and core basins are shown in black colours

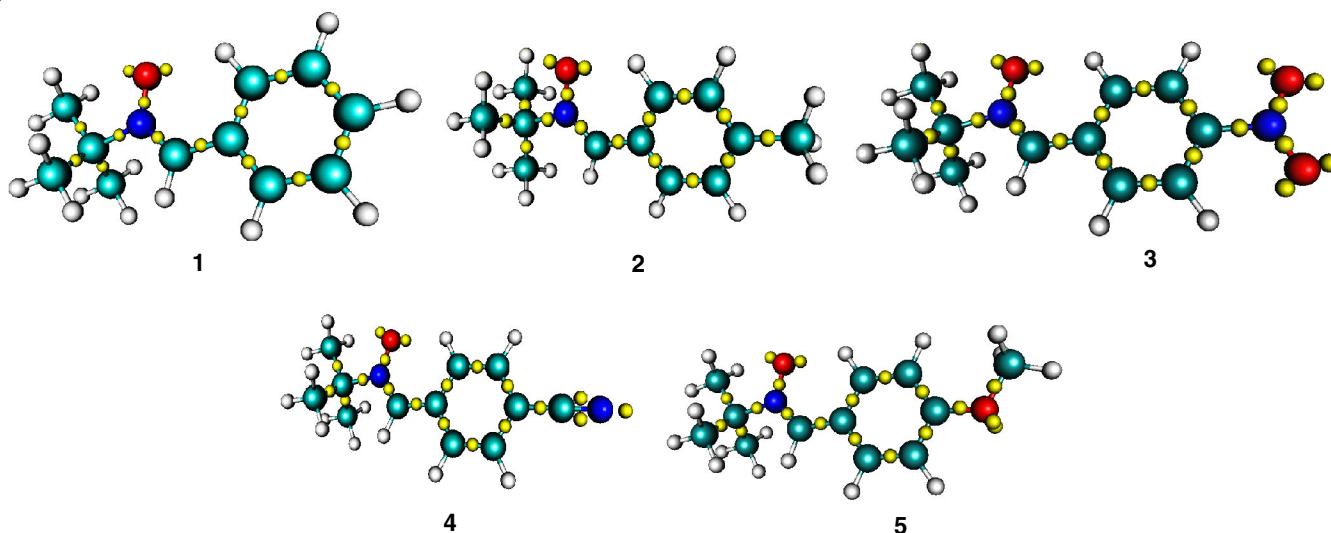


Fig. 2. Basin attractor position of nitrones **1-5**. ELF attractors are shown in yellow colour

TABLE-1
MOST SIGNIFICANT ELF VALENCE BASIN POPULATIONS OF
NITRONES **1-5**. ELF VALENCE BASIN POPULATION ARE
GIVEN IN AVERAGE NUMBER OF ELECTRONS, e

| Nitrone | V(O1) | V'(O1) | V(N2,O1) | V(C3, N2) |
|----------|-------|--------|----------|-----------|
| 1 | 2.86 | 3.01 | 1.38 | 3.80 |
| 2 | 2.89 | 3.01 | 1.37 | 3.79 |
| 3 | 2.85 | 2.97 | 1.40 | 3.72 |
| 4 | 2.85 | 3.02 | 1.38 | 3.68 |
| 5 | 2.87 | 3.06 | 1.34 | 3.77 |

synaptic V(O1) and V'(O1) basins integrating at a total population of 5.87e, 5.90e, 5.82e, 5.87e and 5.93e, which were associated with the lone-pair electron density at oxygen O1. It is also evident that an electron withdrawing nitro group in **3** decreases the lone pair electron density at O1 compared to unsubstituted nitrone **1**.

Total electron density of monosynaptic V(O1) basin in **4** is higher than that of **1**, owing to the presence of electron dona-

ting OMe substituent. Disynaptic V(N2,O1) integrating at 1.34-1.40e can be associated with the underpopulated N2-O1 bond, while disynaptic V(C3,N2) integrating at 3.68-3.80e can be associated with the underpopulated C3-N2 double bond. Nitrones **1-5** do not show the presence of any *pseudoradical* or carbenoid centre and hence were classified as zwitter-ionic type TACs.

Analysis of CDFT indices of *N-t*-butyl- α -aryl nitrones: Several studies [22] have been devoted to analyze the electronic behaviour of molecular systems in terms of global indices defined with the conceptual density functional theory (CDFT). Global indices of nitrones **1-5** are given in Table-2. The electronic chemical potential (μ) quantifies the propensity of a system to exchange electron density (at its ground state) with the environment. The chemical potential (μ) values of nitrones **1-5** follow the order: **5** > **2** > **1** > **4** > **3**, which shows direct influence of electron demand character of *C*-aryl substituent on the electron density exchange by nitrone.

Global electrophilicity (ω) defined by Domingo *et al.* [36] at B3LYP/6-31G(d) level classifies molecular systems with

TABLE-2
B3LYP/6-31G(d) CALCULATED ELECTRONIC
CHEMICAL POTENTIAL (μ), CHEMICAL HARDNESS (η),
GLOBAL ELECTROPHILICITY (ω) AND GLOBAL
NUCLEOPHILICITY (N) OF THE NITRONES **1-5**

| Nitrone | μ (eV) | η (eV) | ω (eV) | N (eV) |
|----------|------------|-------------|---------------|----------|
| 1 | -3.22 | 4.22 | 1.23 | 3.78 |
| 2 | -3.17 | 4.22 | 1.19 | 3.84 |
| 3 | -4.31 | 3.56 | 2.61 | 3.02 |
| 4 | -3.97 | 3.92 | 2.01 | 3.18 |
| 5 | -2.98 | 4.16 | 1.07 | 4.05 |

$\omega < 0.80$ eV as marginal electrophiles, with 0.80 eV $< \omega < 1.50$ eV as moderate electrophiles and with $\omega > 1.50$ eV as strong electrophiles. Global electrophilicity follows the order **3** $>$ **4** $>$ **1** $>$ **2** $>$ **5**. Nitrones **1**, **2** and **5** are thus classified as moderate electrophiles (Table-2), while nitrones **3** and **4** are classified as strong electrophiles due to the presence of electron withdrawing nitro and cyano *C*-aryl substituents. Nucleophilicity index (N) defined by Domingo [37] for nitrones **1-5** follow the order, **5**

$> \mathbf{2} > \mathbf{1} > \mathbf{4} > \mathbf{3}$, which is just the reverse of electrophilicity index. Thus, *C*-aryl substituents have appreciable influence on the electron demand characteristics of these nitrones.

The calculated Fukui functions for radical attack $f^o(r)$ using natural population analysis (NPA) [38] and Merz-Kollman [39] algorithm for radical attack at oxygen O1 and carbon C3 are listed in Table-3. Natural population analysis (NPA) calculated Fukui function $f^o(r)$ at oxygen O1 of nitrones **1-5** showed a higher values than that at C3 carbon. On contrary, Merz-Kollman calculated Fukui function $f^o(r)$ at carbon C3 was higher than that at O1 oxygen in each case. Experimental studies [8,9] showed a radical attack at C3 carbon of the nitrones. Hence, Merz-Kollman system performs better than the natural population analysis (NPA) calculations for radical attack to *N*-*t*-butyl- α -phenyl nitrone (PBN) and its derivatives.

B3LYP/6-31G(d) optimized geometry of *cis*- and *trans*-hydroxyl, methyl and hydroperoxyl adducts of PBN **1** are shown in Fig. 3 and the relative energy, enthalpy and free energy values of adducts are collected in Table-4. Some appealing conclusions can be drawn from these relative energies.

TABLE-3
B3LYP/6-31G(d) CALCULATED FUKUI FUNCTIONS OF O1 AND C3 SITES OF NITRONES

| Nitrone | MK | | | NPA | | | |
|----------|----|----------|----------|-----|----------|----------|----------|
| | | $f^+(r)$ | $f^-(r)$ | | $f^+(r)$ | $f^-(r)$ | $f^o(r)$ |
| 1 | O1 | 0.145 | 0.218 | O1 | 0.171 | 0.275 | 0.223 |
| | C3 | 0.280 | 0.120 | C3 | 0.140 | 0.159 | 0.150 |
| 2 | O1 | 0.152 | 0.220 | O1 | 0.090 | 0.300 | 0.195 |
| | C3 | 0.322 | 0.119 | C3 | 0.182 | 0.080 | 0.131 |
| 3 | O1 | 0.120 | 0.232 | O1 | 0.098 | 0.278 | 0.188 |
| | C3 | 0.186 | 0.226 | C3 | 0.039 | 0.177 | 0.108 |
| 4 | O1 | 0.142 | 0.223 | O1 | 0.112 | 0.265 | 0.188 |
| | C3 | 0.308 | 0.204 | C3 | 0.076 | 0.156 | 0.116 |
| 5 | O1 | 0.155 | 0.206 | O1 | 0.121 | 0.244 | 0.182 |
| | C3 | 0.346 | 0.105 | C3 | 0.139 | 0.105 | 0.122 |

Analysis of thermodynamic stability of hydroxyl, methyl and hydroperoxyl adducts

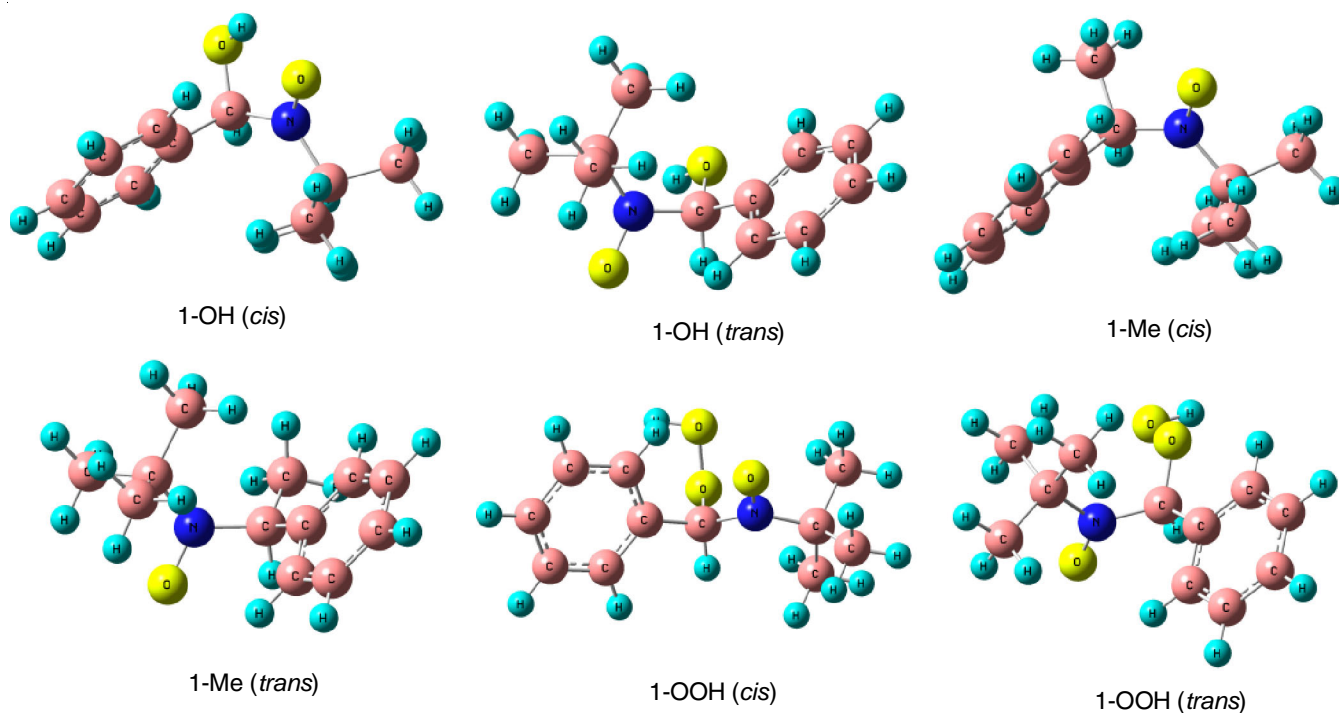


Fig. 3. B3LYP/6-31G(d) optimized geometry of *cis* and *trans* hydroxyl, methyl and hydroperoxyl adducts of PBN **1**

TABLE-4
B3LYP/6-31G(d) OPTIMIZED RELATIVE ENERGIES (kJ mol⁻¹) OF HYDROXYL, METHYL AND HYDROPEROXYL ADDUCTS

| | X = OH | | | X = Me | | | X = OOH | | |
|----------------------|------------|------------|------------|------------|------------|------------|------------|------------|------------|
| | ΔE | ΔG | ΔH | ΔE | ΔG | ΔH | ΔE | ΔG | ΔH |
| 1-X (<i>cis</i>) | -222.7 | -162.8 | -209.3 | -186.3 | -116.0 | -165.8 | -84.6 | -20.5 | -75.8 |
| 1-X (<i>trans</i>) | -210.1 | -150.7 | -196.7 | -164.5 | -91.7 | -144.8 | -83.3 | -23.9 | -74.9 |
| 2-X (<i>cis</i>) | -214.7 | -159.1 | -201.3 | -177.5 | -114.0 | -159.1 | -77.9 | -23.0 | -69.5 |
| 2-X (<i>trans</i>) | -201.8 | -150.3 | -188.8 | -156.1 | -85.4 | -139.8 | -74.5 | -21.3 | -66.1 |
| 3-X (<i>cis</i>) | -210.1 | -155.3 | -197.2 | -175.4 | -111.0 | -157.0 | -70.7 | -13.4 | -62.4 |
| 3-X (<i>trans</i>) | -200.1 | -145.7 | -187.1 | -152.8 | -86.7 | -134.8 | -68.7 | -16.3 | -60.7 |
| 4-X (<i>cis</i>) | -210.6 | -156.1 | -197.6 | -175.8 | -111.0 | -157.4 | -66.1 | -10.0 | -60.7 |
| 4-X (<i>trans</i>) | -198.8 | -145.7 | -185.9 | -153.2 | -86.2 | -134.4 | -69.5 | -12.2 | -62.0 |
| 5-X (<i>cis</i>) | -212.6 | -158.6 | -199.3 | -175.0 | -111.0 | -156.6 | -75.8 | -17.2 | -67.4 |
| 5-X (<i>trans</i>) | -200.1 | -145.3 | -186.7 | -154.0 | -87.5 | -135.2 | -72.4 | -19.7 | -64.5 |

(a) Formation of hydroxyl, methyl and hydroperoxyl radical adducts was highly exothermic in each case (Table-4), which justifies the spin trapping efficiency of PBN derivatives.

(b) Hydroxyl adducts were more stable than methyl and hydroperoxyl adducts. Hydroperoxyl adducts were the least stable adducts along the series. Relative energy of hydroxyl adducts were stabilized than methyl adducts by 34.7 to 47.3 kJ mol⁻¹. Differences in relative enthalpy and free energies of hydroxyl and methyl adducts are 40.2-52.3 and 44.3-64.9 kJ mol⁻¹. Relative energy of hydroxyl adducts were stabilized than hydroperoxyl adducts by 126.8 to 144.5 kJ mol⁻¹. The corresponding differences in enthalpy and free energy of hydroxyl and hydroperoxyl adducts were 121.8–136.9 and 125.6–146.1 kJ mol⁻¹.

(c) For hydroxyl radical, the *cis*-adducts were more stable than the *trans*-adducts in each case by energy difference of 10.0 to 12.9 kJ mol⁻¹, enthalpy difference of 10.1 to 12.6 kJ mol⁻¹ and free energy difference of 8.8 to 13.3 kJ mol⁻¹. For methyl radical, the *cis*-adducts were also more stable than *trans*-adducts, but with a higher energy difference compared to that in hydroxyl adducts. The *cis*- and *trans*-methyl adducts differ by the energy difference of 21.0 to 22.6 kJ mol⁻¹, enthalpy difference of 19.3 to 22.2 kJ mol⁻¹ and free energy difference of 23.5 to 28.6 kJ mol⁻¹. For hydroperoxyl radical, *cis*- and *trans*-adduct stabilities were comparable and differed minimally with the energy difference of 1.3 to 3.4 kJ mol⁻¹, enthalpy difference of 0.9 to 3.4 kJ mol⁻¹ and a free energy difference of 1.7 to 2.5 kJ mol⁻¹.

Analysis of solvent effects: Relative energies of optimized hydroxyl, methyl and hydroperoxyl adducts in different solvents are shown in Figs. 4-6. Eight solvents *viz.* water, methanol, DMSO, acetone, dichloromethane, toluene, CCl₄ and heptane were selected for the study, allowing a progressive decrease in polarity from water to heptane. Relative energies of hydroxyl adducts were in the range -185 to -225 kJ mol⁻¹, methyl adducts were -150 to -190 kJ mol⁻¹ and hydroperoxyl adducts were -85 to -50 kJ mol⁻¹. Stability order of adducts, hydroxyl > methyl > hydroperoxyl was observed in each solvent for both *cis*- and *trans*-adducts. Stability of adducts increases from water to heptane and finally, gas phase adducts attain the highest stability in each series. Appreciable decrease in relative energy was observed from dichloromethane to toluene (Fig. 4). For *cis*-hydroxyl adduct, relative energies in dichloromethane and toluene solvents differed by 10.5, 9.4, 8.8, 8.0 and 9.9 kJ mol⁻¹, respectively for nitrones 1-5. The corresponding differences in case of *trans*-

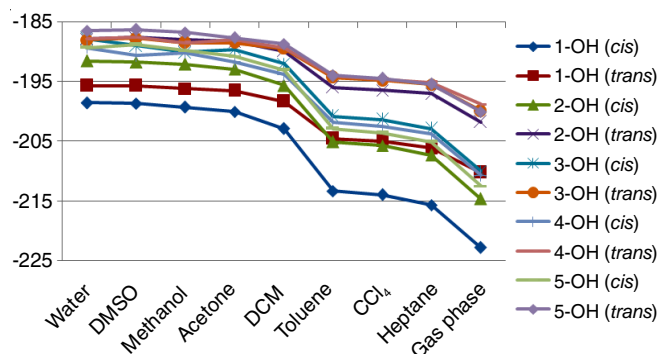


Fig. 4. B3LYP/6-31G(d) calculated relative energies (kJ mol⁻¹) of *cis* and *trans* hydroxyl adducts of nitrones 1-5 in different solvents

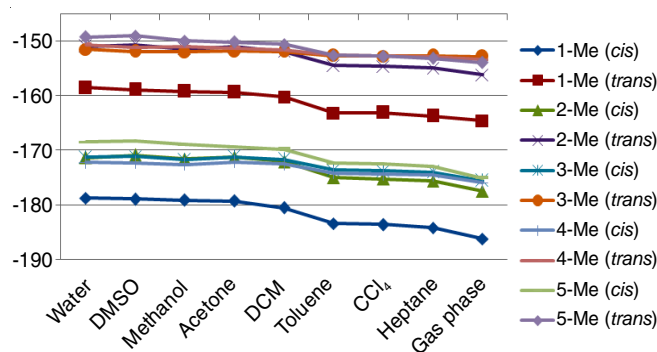


Fig. 5. B3LYP/6-31G(d) calculated relative energies (kJ mol⁻¹) of *cis* and *trans* methyl adducts of nitrones 1-5 in different solvents

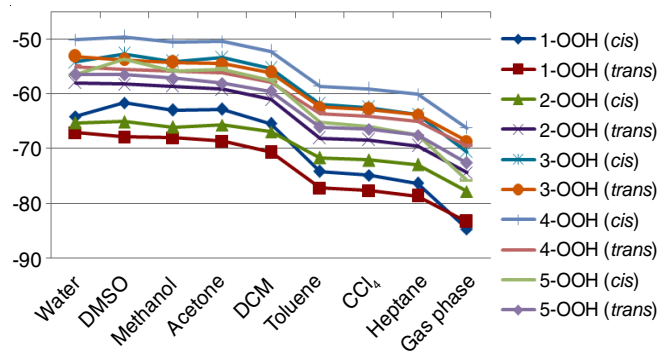


Fig. 6. B3LYP/6-31G(d) calculated relative energies (kJ mol⁻¹) of *cis* and *trans* hydroperoxyl adducts of nitrones 1-5 in different solvents

hydroxyl adducts were 6.3, 6.1, 4.8, 4.7 and 5.3 kJ mol⁻¹. On the other hand, *cis*-methyl adducts in dichloromethane were destabilized than toluene by 2.8, 2.9, 1.9, 1.6 and 2.5 kJ mol⁻¹, respectively for nitrones 1-5 and this difference was 0.7-2.9

kJ mol^{-1} for *trans*-methyl adducts. Difference in relative energies of *cis*-hydroperoxyl adducts in dichloromethane and toluene was 8.7–4.7 kJ mol^{-1} and for *trans*-hydroperoxyl adducts was 5.8–7.1 kJ mol^{-1} . Thus, the stability of hydroxyl adducts showed a higher dependence on solvent polarity compared to methyl and hydroperoxyl adducts. Stability of *cis*-adducts relative to the *trans*-adducts was highest for methyl radical, while for hydroperoxyl radical, comparable energies of *cis*- and *trans*-adducts was observed in some cases.

Conclusion

Radical capture by *N*-*t*-butyl- α -aryl nitrones was analyzed by using DFT calculations. The studied nitrones **1–5** did not contain any *pseudoradical* or carbenoid centre and therefore classified as zwitter-ionic type three atom components by the topological analysis of electron localization function (ELF). Global CDFT indices of nitrones were influenced considerably by the electron demand character of the *C*-aryl substituents. Merz-Kollman algorithm provides correct site selectivity for radical attack at carbon atom unlike the natural population analysis. Stability of adducts follows the order: hydroxyl > methyl > hydroperoxyl. *cis*-Adducts were more stable than *trans*-adducts in case of hydroxyl and methyl radicals, while their relative energies for hydroperoxyl radical capture were comparable. Stability of adducts decreased with increase in polarity of the solvent in each case.

ACKNOWLEDGEMENTS

The authors are thankful to Retd. Prof. Manas Banerjee, University of Burdwan, India for fruitful suggestions.

CONFLICT OF INTEREST

The authors declare that there is no conflict of interests regarding the publication of this article.

REFERENCES

1. A. Phaniendra, D.B. Jestadi, and L. Periyasamy, *Indian. J. Clin. Biochem.*, **30**, 11 (2015); <https://doi.org/10.1007/s12291-014-0446-0>
2. C. C. Benz and C. Yau, *Nat. Rev. Cancer.*, **8**, 875 (2008); <https://doi.org/10.1038/nrc2522>
3. L. M. Sayre, G. Perry and M. A. Smith, *Chem. Res. Toxicol.*, **21**, 172 (2008); <https://doi.org/10.1021/tx700210j>
4. R. A. Cohen and X. Tong, *J. Cardiovasc. Pharmacol.*, **55**, 308 (2010); <https://doi.org/10.1097/fjc.0b013e3181d89670>
5. A. Nawab, A. Nichols, R. Klug, J. I. Shapiro and K. Sodhi, *J Clin Cell Immunol.*, **8**, 505, (2017); <https://doi.org/10.4172/2155-9899.1000505>
6. G.B. Gonzalez, C. Aliaga, C.O. Azar, M.C.Z.-Lopez, M. Gonzalez and H. Cerecetto, *Curr. Org. Chem.*, **21**, 2062 (2017); <https://doi.org/10.2174/1385272821666170228131324>
7. R.A. Floyd, H.K. Chandru, T. He and R. Towner, *Anticancer Agents Med. Chem.*, **11**, 373 (2011); <https://doi.org/10.2174/1871520117956677517>
8. Y. Kotake and E.G. Janzen, *J. Am. Chem. Soc.*, **113**, 9503 (1991); <https://doi.org/10.1021/ja00025a013>
9. E.G. Janzen, Y. Kotake and R.D. Hinton, *Free Radical. Biol. Med.*, **12**, 169 (1992); [https://doi.org/10.1016/0891-5849\(92\)90011-5](https://doi.org/10.1016/0891-5849(92)90011-5)
10. K. Makino, T. Hagiwara and A. Murakami, *Radiat. Phys. Chem.*, **37**, 657 (1991); [https://doi.org/10.1016/1359-0197\(91\)90164-W](https://doi.org/10.1016/1359-0197(91)90164-W)
11. S.E. Bottle and A.S. Micallef, *Org. Biomol. Chem.*, **1**, 2581 (2003); <https://doi.org/10.1039/B300642E>
12. N. Vrbjar, S. Zöllner, R.F. Haseloff, M. Pissarek and I.E. Blasig, *Mol. Cell. Biochem.*, **186**, 107–115 (1998); <https://doi.org/10.1023/A:1006875515357>
13. P.A. Lapchak, D.F. Chapman and J.A. Zivin, *Stroke*, **32**, 147 (2001); <https://doi.org/10.1161/01.STR.32.1.147>
14. D.N. Polovyanenko, V.F. Plyusnin, V.A. Reznikov, V.V. Khramtsov and E.G. Bagryanskaya, *J. Phys. Chem. B.*, **112**, 4841 (2008); <https://doi.org/10.1021/jp711548x>
15. V. Marchand, N. Charlier, J. Verrax, P. BucCalderon, P. Levêque and B. Gallez, *PLoS ONE.*, **12**, e0172998 (2017); <https://doi.org/10.1371/journal.pone.0172998>
16. P. D. Sawant, *Cosmetics.*, **5**, 8 (2018); <https://doi.org/10.3390/cosmetics5010008>
17. F.A. Villamena, C.M. Hadad and J.L. Zweier, *J. Am. Chem. Soc.*, **126**, 1816 (2004); <https://doi.org/10.1021/ja038838k>
18. F.A. Villamena, C.M. Hadad, and J.L. Zweier., *J. Phys. Chem. A.*, **109**, 1662 (2005); <https://doi.org/10.1021/jp0451492>
19. S.-U. Kim and F.A. Villamena, *J. Phys. Chem. A.*, **116**, 886 (2012); <https://doi.org/10.1021/jp209896n>
20. A.D. Becke and K.E. Edgecombe, *J. Chem. Phys.*, **92**, 5397 (1990); <https://doi.org/10.1063/1.458517>
21. B. Silvi and A. Savin, *Nature.*, **371**, 683 (1994); <https://www.nature.com/articles/371683a0>
22. L.R. Domingo, M. Ríos-Gutiérrez and P. Pérez, *Molecules.*, **21**, 748 (2016); <https://doi.org/10.3390/molecules21060748>
23. A.D. Becke, *Phys. Rev. A.*, **38**, 3098 (1988); <https://doi.org/10.1103/PhysRevA.38.3098>
24. C. Lee, W. Yang and R.G. Parr, *Phys. Rev. B.*, **37**, 785 (1988); <https://doi.org/10.1103/PhysRevB.37.785>
25. H.B. Schlegel, *J. Comput. Chem.*, **3**, 214 (1982); <https://doi.org/10.1002/jcc.540030212>
26. H.B. Schlegel, ed.: D.R. Yarkony, Modern Electronic Structure Theory, World Scientific Publishing: Singapore (1994).
27. J. Tomasi and M. Persico, *Chem. Rev.*, **94**, 2027 (1994); <https://doi.org/10.1021/cr00031a013>
28. E. Cancés, B. Mennucci and J. Tomasi, *Chem. Phys.*, **107**, 3032 (1997); <https://doi.org/10.1063/1.474659>
29. V. Barone, M. Cossi and J. Tomasi, *J. Comput. Chem.*, **19**, 404 (1998); [https://doi.org/10.1002/\(SICI\)1096-987X\(199803\)19:4<404::AID-JCC3>3.0.CO;2-W](https://doi.org/10.1002/(SICI)1096-987X(199803)19:4<404::AID-JCC3>3.0.CO;2-W)
30. T. Lu and F. Chen, *J. Comput. Chem.*, **33**, 580 (2012); <https://doi.org/10.1002/jcc.22885>
31. W. Humphrey, A. Dalke and K. Schulten, *J. Molec. Graphics.*, **14**, 33 (1996); [https://doi.org/10.1016/0263-7855\(96\)00018-5](https://doi.org/10.1016/0263-7855(96)00018-5)
32. E.F. Pettersen, T.D. Goddard, C.C. Huang, G.S. Couch, D.M. Greenblatt, E.C. Meng and T.E. Ferrin, *J. Comput. Chem.*, **25**, 1605 (2004); <https://doi.org/10.1002/jcc.20084>
33. M.J. Frisch, G.W. Trucks, H.B. Schlegel, G.E. Scuseria, M.A. Robb, J.R. Cheeseman, G. Scalmani, V. Barone, B. Mennucci, G.A. Petersson, H. Nakatsuji, M. Caricato, X. Li, H.P. Hratchian, A.F. Izmaylov, J. Bloino, G. Zheng, J.L. Sonnenberg, M. Hada, M. Ehara, K. Toyota, R. Fukuda, J. Hasegawa, M. Ishida, T. Nakajima, Y. Honda, O. Kitao, H. Nakai, T. Vreven, J.A. Montgomery Jr., J.E. Peralta, F. Ogliaro, M. Bearpark, J.J. Heyd, E. Brothers, K.N. Kudin, V.N. Staroverov, R. Kobayashi, J. Normand, K. Raghavachari, A. Rendell, J.C. Burant, S.S. Iyengar, J. Tomasi, M. Cossi, N. Rega, J.M. Millam, M. Klene, J.E. Knox, J.B. Cross, V. Bakken, C. Adamo, J. Jaramillo, R. Gomperts, R.E. Stratmann, O. Yazyev, A.J. Austin, R. Cammi, C. Pomelli, J.W. Ochterski, R.L. Martin, K. Morokuma, V.G. Zakrzewski, G.A. Voth, P. Salvador, J.J. Dannenberg, S. Dapprich, A.D. Daniels, Ö. Farkas, J.B. Foresman, J.V. Ortiz, J. Cioslowski and D.J. Fox, Gaussian Inc., Wallingford CT, Gaussian 09, Revision D.01 (2009).
34. L.R. Domingo, *Molecules*, **21**, 1319 (2016); <https://doi.org/10.3390/molecules21101319>
35. M.R. Gutierrez and L.R. Domingo, *Eur. J. Org. Chem.*, **2**, 267 (2019); <https://doi.org/10.1002/ejoc.201800916>
36. L.R. Domingo, M.J. Aurell, P. Perez and R. Contreras, *Tetrahedron*, **58**, 4417 (2002); [https://doi.org/10.1016/S0040-4020\(02\)00410-6](https://doi.org/10.1016/S0040-4020(02)00410-6)
37. L.R. Domingo, E. Chamorro and P. Pérez, *J. Org. Chem.*, **73**, 4615 (2008); <https://doi.org/10.1021/jo800572a>
38. A.E. Reed, R.B. Weinstock and F. Weinhold, *J. Chem. Phys.*, **83**, 735 (1985); <https://doi.org/10.1063/1.449486>
39. B.H. Besler, K.M. Jr. Merz and P.A. Kollman, *J. Comput. Chem.*, **11**, 431 (1990); <https://doi.org/10.1002/jcc.540110404>